THE JOURNAL OF BIOLOGICAL CHEMISTRY VOL. 290, NO. 11, pp. 7040–7053, March 13, 2015

Dysfunction of Platelet-derived Growth Factor Receptor α (PDGFRα) Represses the Production of Oligodendrocytes from Arylsulfatase A-deficient Multipotential Neural Precursor Cells*

Received for publication, January 5, 2015 Published, JBC Papers in Press, January 20, 2015, DOI 10.1074/jbc.M115.636498

Katarzyna C. Pituch[‡], Ana L. Moyano[‡], Aurora Lopez-Rosas[‡], Felecia M. Marottoli[‡], Guannan Li[§], Chenqi Hu[§], Richard van Breemen[§], Jan E. Månsson[¶], and Maria I. Givogri[‡1]

From the [‡]Department of Anatomy and Cell Biology, College of Medicine, and the [§]Department of Medical Chemistry and Pharmacognosy, College of Pharmacy, University of Illinois, Chicago, Illinois 60612 and the [¶]Department of Clinical Chemistry, Sahlgren Academy, University of Gothenburg, SE-413 45 Gothenburg, Sweden

Background: PDGFRα is a key signaling component in oligodendrogenesis.
Results: Multipotential Neural precursors (NPs) deficient in arylsulfatase A (ASA) show a higher ratio of long *versus* short fatty acid sulfatides, reduction in PDGFRα, decreased AKT phosphorylation, and increased exosomal shedding of PDGFRα.
Conclusion: Sulfatides are regulators of NP response to PDGF-AA.
Significance: A novel regulatory mechanism of PDGFRα signaling is described.

The membrane-bound receptor for platelet-derived growth factor A (PDGFRα) is crucial for controlling the production of oligodendrocytes (OLs) for myelination, but regulation of its activity during OL differentiation is largely unknown. We have examined the effect of increased sulfated content of galactosylceramides (sulfatides) on the regulation of PDGFRα in multipotential neural precursors (NPs) that are deficient in arylsulfatase A (ASA) activity. This enzyme is responsible for the lysosomal hydrolysis of sulfatides. We show that sulfatide accumulation significantly impacts the formation of OLs via deregulation of PDGFRα function. PDGFRα is less associated with detergent-resistant membranes in ASA-deficient cells and showed a significant decrease in AKT phosphorylation. Rescue experiments with ASA showed a normalization of the ratio of long *versus* short sulfatides, restored PDGFRα levels, corrected its localization to detergent-resistant membranes, increased AKT phosphorylation, and normalized the production of OLs in ASA-deficient NPs. Moreover, our studies identified a novel mechanism that regulates the secretion of PDGFRα in NPs, in glial cells, and in the brain cortex via exosomal shedding. Our study provides a first step in understanding the role of sulfatides in regulating PDGFRα levels in OLs and its impact in myelination.

Oligodendrocyte progenitor cells (OPCs)[2] are primarily generated from undifferentiated multipotential neural precursors (NPs) during early embryogenesis under the influence of morphogenic molecules, such as Shh (sonic hedgehog) (1–4). Multiple mechanisms are developmentally coordinated to regulate the differentiation of OPCs into functional oligodendrocytes (OLs) (5–7). Of these, signaling through the platelet-derived growth factor receptor α (PDGFRα) is essential in controlling the proliferation and survival of OPCs (8–10). PDGFRα is expressed in NPs (11) and marks the appearance of the first PDGF-responsive OPCs during early neurogliogenesis (12). Numerous studies have highlighted the relevance of PDGFRα signaling in oligodendrogenesis. For example, PDGFRα$^+$ cells isolated from the embryonic spinal cord exclusively generate myelinating oligodendrocytes (12, 13). Furthermore, the formation of mature OLs is significantly reduced upon ablation of PDGFRα$^+$ cells (12) and in mice with targeted disruption of its ligand, PDGF-AA (14). Functionally, the activity of PDGFRα depends in part on its localization to detergent-resistant membrane (DRM) domains in the plasma membrane and interaction with integrin complexes (15–17). The association of PDGFRα with DRMs underlines the possibility that conditions affecting DRMs may impact PDGFRα function and, therefore, the myelination program.

Previously, we found that exogenous sulfated galactosylceramides (sulfatides) significantly reduced the formation of OLs from NPs *in vitro* (18). One interpretation from these results is that sulfatides might repress the sensitivity of OPCs to proliferating signals such as PDGF-AA, thereby reducing the pool of progenitors available for differentiation into mature OLs. Sulfatides are crucial sphingolipids in myelin architecture (19) and have been found to negatively regulate the maturation of OPCs into differentiated OLs (20, 21), but the mechanism is still unknown. Sphingolipids, including sulfatides, have structural

* This work was supported, in whole or in part, by National Institutes of Health Ruth L. Kirschstein National Research Service Award F31 (to K. P. C.). This work was also supported by National Multiple Sclerosis Society Grants PP1516 and RG 4439-A-2 and by Department of Defense Contract W81XWH-11-1-0198 (to M. I. G.).

[1] To whom correspondence should be addressed: Dept. of Anatomy and Cell Biology, College of Medicine, University of Illinois, 808 S. Wood St. M/C 512, Chicago, IL 60612. Tel.: 312-413-1072; E-mail: mgivogri@uic.edu.

[2] The abbreviations used are: OPC, oligodendrocyte progenitor cell; NP, neural precursor; OL, oligodendrocyte; PDGFRα, platelet-derived growth factor receptor α; DRM, detergent-resistant membrane; DIV, days *in vitro*; UHPLC, ultrahigh pressure liquid chromatography; EGFR, epidermal growth factor receptor; GFAP, glial fibrillary acidic protein; MBP, myelin basic protein; PLP, proteolipid protein; ASA, arylsulfatase A; ASACM, ASA conditioned medium; GM1, monosialotetrahexosylganglioside.

and functional roles in DRMs (22, 23) and participate in caveolar and exosomal biogenesis (22, 24–26). Therefore, sulfatides have an intrinsic potential to modulate the activity of membrane-bound receptors such as PDGFRα by altering membrane domains such as DRMs.

In this study, we tested the hypothesis that sulfatides contribute to the regulation of oligodendrogenesis by modulating PDGFRα function. We found that increased sulfatide levels in NPs lead to a reduced production of OPCs and OLs. Furthermore, we observed a diminished association of PDGFRα with DRMs, repressed AKT phosphorylation, and exacerbated secretion of PDGFRα via exosomes. We present evidence that exosomal secretion of PDGFRα is a natural process in glial cells *in vitro* and during myelination of the murine cortex, when sulfatides are highly produced.

EXPERIMENTAL PROCEDURES

Animals—Heterozygous $ASA^{+/-}$ breeders (obtained from Dr. Gieselmann and back-crossed in the C56BL/6 background) were maintained in standard housing conditions, under the approval of the Animal Care and Use Committee. $ASA^{+/+}$ and $ASA^{-/-}$ embryos at 16.5 days of gestation and 3-day-old newborns were used in our experiments. $ASA^{+/+}$ and $ASA^{-/-}$ mice at 7, 14, and 21 days were killed without sex distinctions for immunocytochemical and *in vivo* exosome isolation studies.

Multipotential Neural Precursor Preparations and Cell Culture Conditions—NPs were isolated from $ASA^{+/+}$ and $ASA^{-/-}$ embryonic day 16.5 telencephalon by mechanical dissociation and maintained as proliferating spheres in the presence of 10 ng/ml FGF-2 and 20 ng/ml EGF (27). Cultures of NPs obtained from different litters were used between passages 3 and 10 with identical results ($n = 5–6$). For differentiation assays, NPs were mechanically dissociated and seeded at a density of 7.5×10^4 cells/cm^2 onto coverslips precoated with Matrigel (BD Biosciences) for 1 h at room temperature. Cultures were maintained for 3 or 7 days (3 or 7 DIV) in the absence of growth factors and in the presence of 2% fetal bovine serum (differentiated medium). Differentiated medium containing 2% FBS showed traces of Alix and Rab5B (data not shown). In some experiments, differentiated cells were exposed to PDGF-AA (Peprotech) at a concentration of 20 ng/ml for 1 day after plating. For Western blot analyses, NP spheres were collected 5 days after proliferation or 7 days after plating for differentiation.

Studies of PDGFRα Proteolysis—Analysis of proteolytic degradation of the PDGFRα were performed utilizing 2×10^6 dissociated $ASA^{+/+}$ and $ASA^{-/-}$ NPs. NPs were exposed to 10 μM MG132 or 10 mM NH4CL in basal proliferating medium conditions. Cells incubated with MG132 or NH4Cl for 6 h were collected for protein expression analysis of the PDGFRα as described below (see "Immunoblotting"). Because MG132 was dissolved in DMSO, DMSO-treated $ASA^{+/+}$ and $ASA^{-/-}$ NPs were included as controls. All experiments were repeated three times. Additionally, three independent experiments were performed exposing 4×10^6 dissociated $ASA^{+/+}$ and $ASA^{-/-}$ NPs to PDGF-AA ligand at a concentration of 20 ng/ml for 30 min before cell collection. For these experiments, NPs were starved for 3 h of growth factors present in the proliferating medium (EGF and basic FGF) and exposed to MG132 or NH_4Cl as described above. After starvation, NP metabolism was slowed down by an ice bath for 15 min, cells were pelleted, and medium was preserved on ice. Pelleted NPs were exposed to fresh medium containing PDGF-AA for 30 min on ice. Cells were pelleted and washed to remove unbound ligand and resuspended in their original medium with MG132 or NH_4Cl for an additional 30 min at 37 °C. NPs were pelleted, washed with PBS, and collected for Western blot analysis. NP pellets were analyzed for PDGFRα and downstream signaling for AKT, phospho-AKT (Ser^{308} and Thr^{478}), MAPK p42/44, and phospho-MAPK p42/44 (Thr^{202}/Tyr^{204}).

Sulfatide Treatment—For analysis of the effects of exogenous sulfatides (Avanti), $ASA^{+/+}$ NP spheres were dissociated and incubated with two pulses of 10 μM sulfatides at days 1 and 3 and collected after 5 days.

Mouse Glial Primary Culture—Primary glial cultures were prepared from $ASA^{+/+}$ and $ASA^{-/-}$ as described previously (28). Cell suspensions were seeded in 75-cm^2 tissue culture flasks coated with 10 μg/ml poly-L-lysine at equal cell densities. Medium was changed 4 days after plating. Glial conditioned medium was collected at 7, 14, and 21 DIV and stored at −20 °C.

CG4 Cell Culture—CG4 cells were cultured as described previously (29), except that B104 conditioned medium was replaced with 10 ng/ml PDGFA (BD Biosciences) and 5 ng/ml basic FGF (Peprotech). After 5 days in culture, supernatants were processed for exosomal isolation and cell pellets for Western blot analysis as described below.

Detergent-resistant Membranes Isolation—NP lysates (equivalent to 2 mg of protein) were equilibrated with a solution of 90% sucrose to give a final solution of 45% sucrose and subjected to ultracentrifugation using a sucrose gradient (24). Twelve 0.25-ml fractions were collected and analyzed by immunoblotting.

Cholesterol Assay—Cholesterol levels of $ASA^{+/+}$ and $ASA^{-/-}$ NPs from each sucrose fraction (50 μl) were measured using the fluorometric Amplex Red cholesterol assay kit (Invitrogen). Fluorometric analysis was performed using the Beckman Coulter DTX 880 multimode detector.

Isolation and Analysis of Sulfatides by Ultrahigh Performance Liquid Chromatography Tandem Mass Spectrometry (UHPLC-MS/MS)—Sulfatides were extracted from total lysates of NP spheres at 5 days ($ASA^{+/+}$, $ASA^{-/-}$, and $ASA^{-/-}$ NPs treated with two pulses of 5, 15, or 25% ASA conditioned medium (ASACM) at day 1 and 3 of dissociated spheres) and DRM fractions ($ASA^{+/+}$ and $ASA^{-/-}$ NPs) as described previously with some modifications (30–32). C12:0 sulfatide was used as an internal standard (0.5 μM). Fifty-microliter aliquots from each sample were used for protein quantification. Ten volumes of chloroform/methanol ($CHCl_3/CH_3OH$ (2:1, v/v)) were added to each sample and incubated with agitation at room temperature for 2 h. Each sample was filtered, and 0.2 volumes of 0.9% NaCl was added. Mixtures were vortexed and centrifuged at 2000 rpm for 5 min. The lower phase was dried under N_2 at 45 °C. Lipid extracts were dissolved in $CHCl_3$/0.6 N NaOH, CH_3OH (1:1, v/v) and incubated for 2 h at room temperature with agitation. Extracts were washed with water and centrifuged at 2000 rpm. The lower phase was retained, washed with

$CHCl3/CH_3OH/H_2O$ (3:48:47, v/v/v), and centrifuged at 2000 rpm. The lower phase was evaporated, and the dry product was dissolved in $CHCl_3$ (500 ml/10 mg of product). Lipid extracts were fractionated on an SPE-NH_2 column as described (33). Briefly, upon activation with hexane, fractional elution was carried out, and sulfatides were eluted with $CHCl_3/CH_3OH$/3.6 M aqueous $NH_4C_2H_3O_2$ (30:60:8, v/v/v) (as a last fraction), dried with N_2 at 45 °C, and stored at −20 °C until use. Samples were dissolved in 60 ml of 5 mM NH_4HCO_2 in CH_3OH, and 2 ml were injected onto the UPLC column. The four major sulfatide isoforms enriched in white matter (C16:0, C18:0, C24:0, and C24:1) were analyzed using UHPLC-MS/MS on a Shimadzu Nexera/LCMS-8040 triple quadrupole mass spectrometer (Kyoto, Japan). A Waters Acquity UPLC C18 column (2.1 × 50 mm, 1.7 mm) was used to separate sulfatides. The following gradient was used: 0–3 min, from 65 to 83% A; 3–3.5 min, from 83 to 95% A, held at 95% A for 1.5 min (solvent A, CH_3CN; solvent B, 5 mM NH_4HCO_2 in water, pH 4.5). The flow rate was 0.6 ml/min, the autosampler temperature was 20 °C, and the column oven temperature was 45 °C. All analyte measurements were done using negative ion electrospray mass spectrometry with collision-induced dissociation and selected reaction monitoring. Selected reaction monitoring transitions monitored were as follows: C12:0, *m*/*z* 722 to 97; C16:0, *m*/*z* 778 to 97; C18:0, *m*/*z* 806 to 97; C24:1, *m*/*z* 888 to 97; C24:0, *m*/*z* 890 to 97.

Exosome Preparation and Transmission Electron Microscopy—Conditioned media from NPs (3×10^7 cells) and primary glial cultures (3×10^7) ($n = 3$ for each group) were filtered (0.22 μm) and subjected to ultracentrifugation at 100,000 × *g* for 90 min. Pellets were resuspended in cold PBS and ultracentrifuged at 100,000 × *g* for 90 min. Exosome pellets were dissolved in lysis buffer as described below, and equal amounts of proteins (4 μg) were separated by SDS-PAGE and transferred to nitrocellulose, followed by immunodetection of PDGFRα, EGFR, and the exosomal marker Rab-5b. Exosomes were isolated from $ASA^{+/+}$ and $ASA^{-/-}$ brain cortices at 7, 14, and 21 days postnatal as described (34). The final exosomal pellet was subjected to a sucrose gradient centrifugation at 200,000 × *g* for 16 h at 4 °C. A total of seven fractions were collected (fraction a, top; fraction g, bottom). Fractions b, c, and d, enriched in the exosomal marker Rab-5b, were each resuspended in 40 μl of lysis buffer. Western blot analysis was performed on a half of the volume of each fraction. For transmission electron microscopy, exosomes were fixed in 2% paraformaldehyde and stained as described (35). Samples were imaged using a 120-kV transmission electron microscope, JEOL JEM-1220, and equipped with a Gatan Es1000W 11-megapixel CCD camera.

Rescue of ASA Deficiency in $ASA^{-/-}$ NPs—The deficiency in ASA activity in $ASA^{-/-}$ NPs was rescued by cross-correction using ASA-supplemented cell medium (36). Briefly, ASA-secreting HeLa cells were grown in 10% FCS DMEM/F-12 before conditioning. Cells were incubated with serum-free cell medium for 4 days. Conditioned media were filtered through a 0.45-μm filter and kept frozen until use. For correction experiments, 5, 15, or 25% ASACM or 25% control medium (DMEM/F-12 medium) was added to $ASA^{-/-}$ NP culture medium. ASA activity was measured utilizing 4-methylumberyl sulfate derivative substrate as described by Porter *et al.* (37).

Real-time PCR—RNA was purified using TRIzol (Invitrogen) and reverse-transcribed with Superscript III (Invitrogen). SYBR Green-based real-time PCR analysis was performed using primers specific for the PDGFRα sequence. The 60 S acidic ribosomal protein P0 (RPLP0) was used as an internal standard. Primers were optimized on a standard curve with an efficiency between 90 and 110% and a correlation coefficient higher than and 0.990. PCR analysis was calculated using the ΔΔ*Ct* method. The following primers were used: PDGFRα forward, 5′-ATATGATCTTTCTGTGGTTTAA-3′; reverse, 5′-CACTGCTTGGCAGAGCTACCT-3′; RPLP0 forward, 5′-CACGAAGCTAACGACTATCGC-3′; reverse, 5′-CTCTAGGGACTCGTTCGTGC-3′.

Immunoblotting—Samples were homogenized in lysis buffer (25 mM Tris-HCl, pH 7.4, 150 mM NaCl, 5 mM EDTA, 1% Triton, mammalian protease inhibitor mixture, 1 mM PMSF, 1 mM okadaic acid, and 2 mM sodium orthovanadate) on ice for 30 min with vortexing at 10-min intervals. After centrifugation at 10,000 × *g*, 10 μg of protein/sample was loaded onto 4–12% 1.5-mm precast NuPage gels (Invitrogen) and electrophoresed using an XCell Sure-lock vertical electrophoresis system (Invitrogen). After transferring to nitrocellulose membrane, blots were blocked with milk/BSA solution and incubated with the relevant antibodies. Immunoreactive products were detected using peroxidase-labeled secondary antibodies and ECL chemiluminescent substrate (Pierce). Immunoblots were semiquantified using ImageJ analysis software (National Institutes of Health).

Immunocytochemistry and Immunohistochemistry—For differentiation studies, cultures were maintained for 3 or 7 DIV in the absence of growth factors and in the presence of 2% fetal bovine serum. Cells were fixed with 4% paraformaldehyde for 20 min and washed twice with PBS. Cells were incubated with primary antibodies at room temperature for 1 h or overnight at 4 °C, washed extensively with PBS, and then incubated with Alexa-conjugated secondary antibodies (Molecular Probes). Coverslips or chamber slides were mounted with Prolong Gold antifade reagent with DAPI (Invitrogen) and imaged using either DM5500 Q Microscope with a Leica DFC500 camera or Zeiss Meta 510 confocal microscope. Cell counting was performed in the ImageJ software by counting cell-specific markers (NG2 for oligodendrocyte precursor cells, O4 for intermediate oligodendrocytes, glial fibrillary acidic protein (GFAP) for astrocytes, and DAPI for the nuclei). Three images of each coverslip or chamber slide were counted, and all experiments were repeated at least three times with different primary NPs cultures. The cell percentage was calculated for each specific marker with respect to total $DAPI^+$ cells. Brains were collected after perfusion with PBS and 4% paraformaldehyde. Sections were cryoprotected in 20% sucrose, embedded in OCT, and sectioned at 20 μm on a cryostat. Tissue sections were immunostained for myelin basic protein (MBP) and PDGFRα and developed using the diaminobenzidine-ABC kit (Vector Laboratories).

Antibodies—The following antibodies were used in this study: actin (1:3000; Sigma), AKT (1:1000; Cell Signaling), Alix (1:500; Millipore), ASA (1:750; a gift from Dr. V. Gieselmann, Rheinische Friedrich-Wilhelms University, Bonn, Germany), caveolin 1 (1:1000; Cell signaling), EGFR (1:500; Upstate), p44/42 MAPK (1:2000; Cell Signaling), flotillin 2 (1:2000; BD

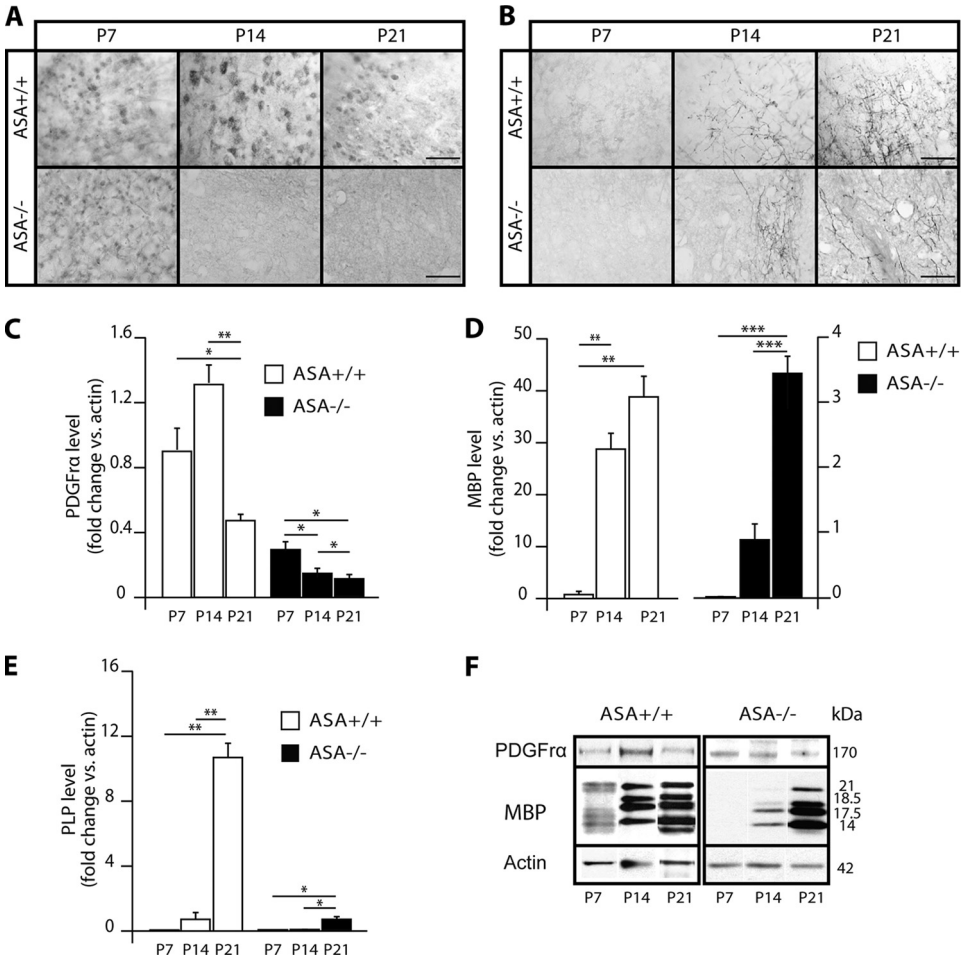

FIGURE 1. **$ASA^{-/-}$ cortex shows a reduction in the expression of PDGFRα.** *A* and *B*, immunocytochemical analysis of PDGFRα and MBP in $ASA^{+/+}$ and $ASA^{-/-}$ cortices. *C–F*, immunoblotting analyses of PDGFRα, MBP, and PLP in mouse cortices at 7, 14, and 21 postnatal days (*P*) showed differing developmentally regulated patterns of expression of these proteins in $ASA^{+/+}$ and $ASA^{-/-}$ cortices. $ASA^{+/+}$ cortex showed a significant reduction in PDGFRα at postnatal day 21, and $ASA^{-/-}$ at postnatal days 14 and 21. MBP expression in $ASA^{-/-}$ cortex showed a 7-day delay during the peak of its expression with respect to $ASA^{+/+}$ cortices (data shown as the mean ± S.E. (*error bars*); $n = 3$). *, $p \leq 0.05$; **, $p \leq 0.01$; ***, $p \leq 0.001$ for $ASA^{-/-}$ or $ASA^{+/+}$ by analysis of variance.

Biosciences), GFAP (1:1000; Millipore), MBP (1:500; a gift from Dr. E. R. Bongarzone (University of Illinois, Chicago, IL)), HSP40 (1:1000; Cell Signaling), HSP60 (1:1000; Cell Signaling), phospho-AKT-Thr^{308} (1:1000; Cell Signaling), phospho-AKT-Ser^{473} (1:1000; Cell Signaling), phospho-p44/42 MAPK (1:1000; Cell Signaling), chondroitin sulfate proteoglycan, NG2 (1:300; Millipore), PDGFRα (1:200; Santa Cruz Biotechnology, Inc., and Cell Signaling), O4 (1:30; a gift from Dr. Bongarzone), proteolipid protein (PLP) (1:50; a gift from Dr. Bongarzone), and Rab-5b (1:200; Santa Cruz Biotechnology).

Statistical Analysis—Data were analyzed by Student's *t* test or one-way analysis of variance, considering a *p* value of <0.05 as significant. Results are given as the means ± S.E. All analyses were performed using GraphPad Prism version 5.0d (GraphPad Software, Inc., La Jolla, CA).

RESULTS

Levels of PDGFRα and Myelin Proteins Are Reduced during Active Myelination in $ASA^{-/-}$ Animals—Previous studies performed in $ASA^{-/-}$ animals during the peak of myelination showed a delayed expression of mRNA for myelin proteins: MBP, myelin and lymphocyte protein, and PLP, which suggests a defect in the differentiation program of OLs in the $ASA^{-/-}$ context (38). We have examined the expression of PDGFRα and MBP by immunohistochemistry in the cortex of $ASA^{+/+}$ and $ASA^{-/-}$ mice during the period of active myelination at postnatal days 7, 14, and 21 (Fig. 1, *A* and *B*). Our analysis showed a reduced content of the PDGFRα (Fig. 1*A*) and MBP (Fig. 1*B*) in the $ASA^{-/-}$ cortex. Immunoblotting analysis confirmed the immunohistochemical findings. PDGFRα protein levels were significantly reduced in the mutant cortex at all ages examined (Fig. 1, *C* and *F*). MBP (Fig. 1, *D* and *F*) and PLP (Fig. 1*E*) were also significantly reduced in the $ASA^{-/-}$ brain.

ASA Deficiency Alters Gliogenesis in Vitro—To better understand the possible effect of ASA deficiency on the production of OLs, multipotential NPs were isolated from embryonic day 16.5 of $ASA^{-/-}$ and $ASA^{+/+}$ mice, and NPs were differentiated for 7 days. $ASA^{-/-}$ NPs produced significantly fewer $O4^+$ intermediate OLs (Fig. 2, *A* and *B*) and more $GFAP^+$ astrocytes (Fig. 2, *A* and *B*) than cells with normal levels of ASA activity. A marked decrease of immature $NG2^+$ OPCs was also determined in $ASA^{-/-}$ cells differentiated for 3 DIV (3.4 ± 0.6% in $ASA^{-/-}$ cells *versus* 8.3 ± 0.5% in $ASA^{+/+}$ cells), indicating that the decrease in the production of oligodendroglial cells starts at

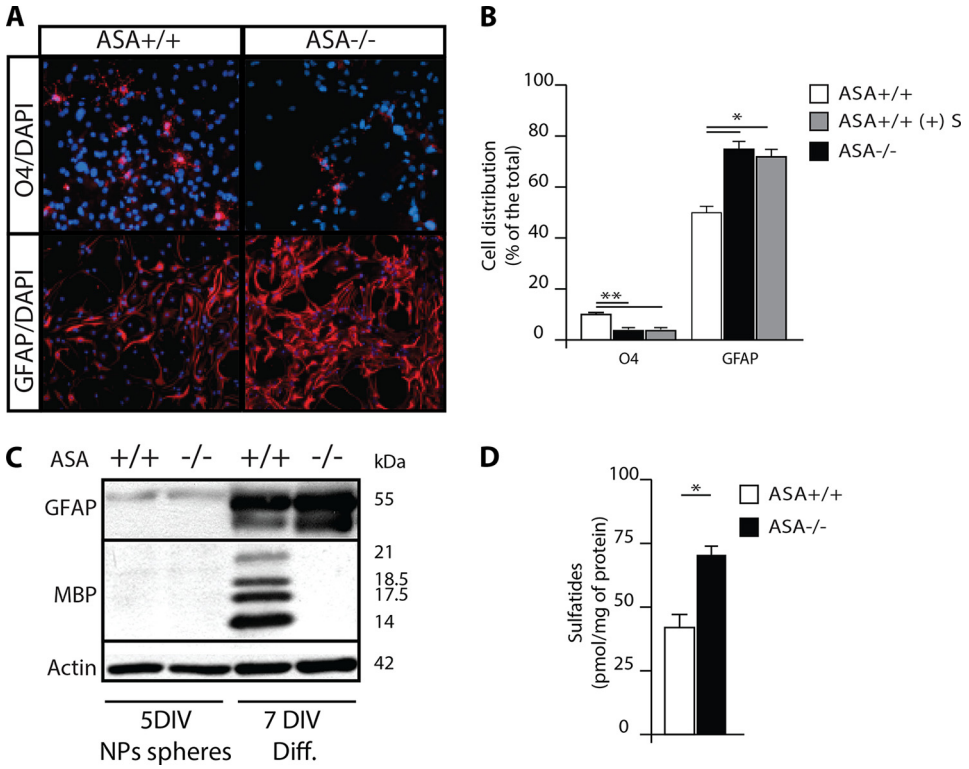

FIGURE 2. **NPs with high sulfatide content generate fewer oligodendrocytes.** *A*, ASA$^{+/+}$ and ASA$^{-/-}$ NPs were differentiated for 7 DIV and immunolabeled with monoclonal antibodies O4 (marker for intermediate OLs, in *red*) and anti-GFAP (marker for astrocytes, in *red*) and counterstained with DAPI (nuclear staining, in *blue*). Representative images of O4^{+} OLs (*top*) and GFAP^{+} astrocytes (*bottom*) are shown. *B*, ASA$^{-/-}$ NPs generate significantly fewer O4^{+} OLs and more GFAP^{+} astrocytes as compared with ASA$^{+/+}$ NPs. Treatment of ASA$^{+/+}$ NPs with sulfatides results in the same effect ($n = 5$; data are shown as the mean ± S.E. (*error bars*)). *, $p < 0.05$ by Student's *t* test. *C*, immunoblot analysis of differentiated ASA$^{+/+}$ and ASA$^{-/-}$ NPs showed a visible reduction in MBP levels in mutant cells as well as significant increases in GFAP. *D*, ASA$^{+/+}$ and ASA$^{-/-}$ NP spheres were analyzed for sulfatide content. ASA$^{-/-}$ NPs showed a significant increase in these sulfatides (data are shown as the mean ± S.E.; $n = 6$). *, $p \leq 0.05$ by Student's *t* test.

early stages of *in vitro* differentiation. Sulfatide-treated ASA$^{+/+}$ NPs showed a significant reduction in the numbers of O4^{+} cells as was observed in differentiated ASA$^{-/-}$ NPs (Fig. 2*B*). Immunoblotting analysis of protein extracts from differentiated ASA$^{-/-}$ NPs confirmed a failure of these cultures to produce OLs that express MBP (Fig. 2*C*). Measurement of four major sulfatide isoforms by UHPLC-MS/MS showed a 2-fold significant increase in sulfatides in ASA$^{-/-}$ NP spheres with respect to ASA$^{+/+}$ NP spheres (Fig. 2*D*).

The PDGFRα Pathway Is Defective in ASA$^{-/-}$ Cells—Because the PDGFRα is a critical signal for the generation of OPCs and their timely maturation into OLs, we studied its expression in ASA$^{-/-}$ NPs. PDGFRα is crucial for regulating the number and survival of OPCs/OL during myelination (9–11, 39–41), mainly by regulating the activity of the AKT or ERK1/2 pathway (42–44). To determine whether this receptor was involved in the phenotype of ASA$^{-/-}$ cells, various experiments were performed. Immunoblotting analyses showed a significant reduction of PDGFRα protein levels in proliferating and differentiating ASA$^{-/-}$ cells (Fig. 3*A*). This decrease appeared specific to PDGFRα because control experiments did not show significant changes in levels of EGFR (Fig. 3*A*). Next, we measured the response of ASA$^{-/-}$ cells to the mitogenic stimulus of exogenous PDGF-AA. Differentiating ASA$^{-/-}$ and ASA$^{+/+}$ NP cultures were incubated in the presence of PDGF-AA and pulsed with BrdU on day 2. Immunocytochemistry of NG2 showed significantly fewer BrdU^{+}/NG2^{+} OPCs in ASA$^{-/-}$ cultures (Fig. 3*B*). Immunoblotting analysis of PDGFRα levels showed reduced levels of the receptor in PDGF-AA-stimulated NPs (Fig. 3*C*), confirming a failure of ASA$^{-/-}$ cells to respond to the growth factor. Functional studies of PDGFRα looking at AKT and MAPK ERK1/2 phosphorylation (Fig. 3, *D–F*) confirmed a severe failure of ASA$^{-/-}$ cells to phosphorylate serine 473 and threonine 308 residues of AKT upon stimulation with PDGF-AA (Fig. 3*E*).

The Transcription and Degradation of the PDGFRα Are Not Affected in ASA$^{-/-}$ Cells—Our previous experiments indicated a reduction of PDGFRα in ASA$^{-/-}$-deficient NPs. This reduction could be caused by different defects affecting protein production (*e.g.* gene transcription), degradation (*e.g.* proteosome), and secretion (45–47). Real-time PCR analyses of PDGFRα mRNA levels (Fig. 4*A*) and immunoblotting analyses for stress response markers (heat shock proteins HSP40 and HSP60; not shown) did not find significant differences in ASA$^{-/-}$ and ASA$^{+/+}$ NPs. Furthermore, blockage of proteasome activity with MG132 and of lysosomal function with NH4Cl showed no significant differences in PDGFRα protein levels in ASA$^{-/-}$ cells grown in basal culture conditions or stimulated with PDGF-AA (Fig. 4, *B* and *C*). Together, these results indicate that defects in gene transcription, stress-related gene translation deficiencies, and altered protein degradation are unlikely to be causes for the reduction of PDGFRα protein levels in ASA$^{-/-}$ cells.

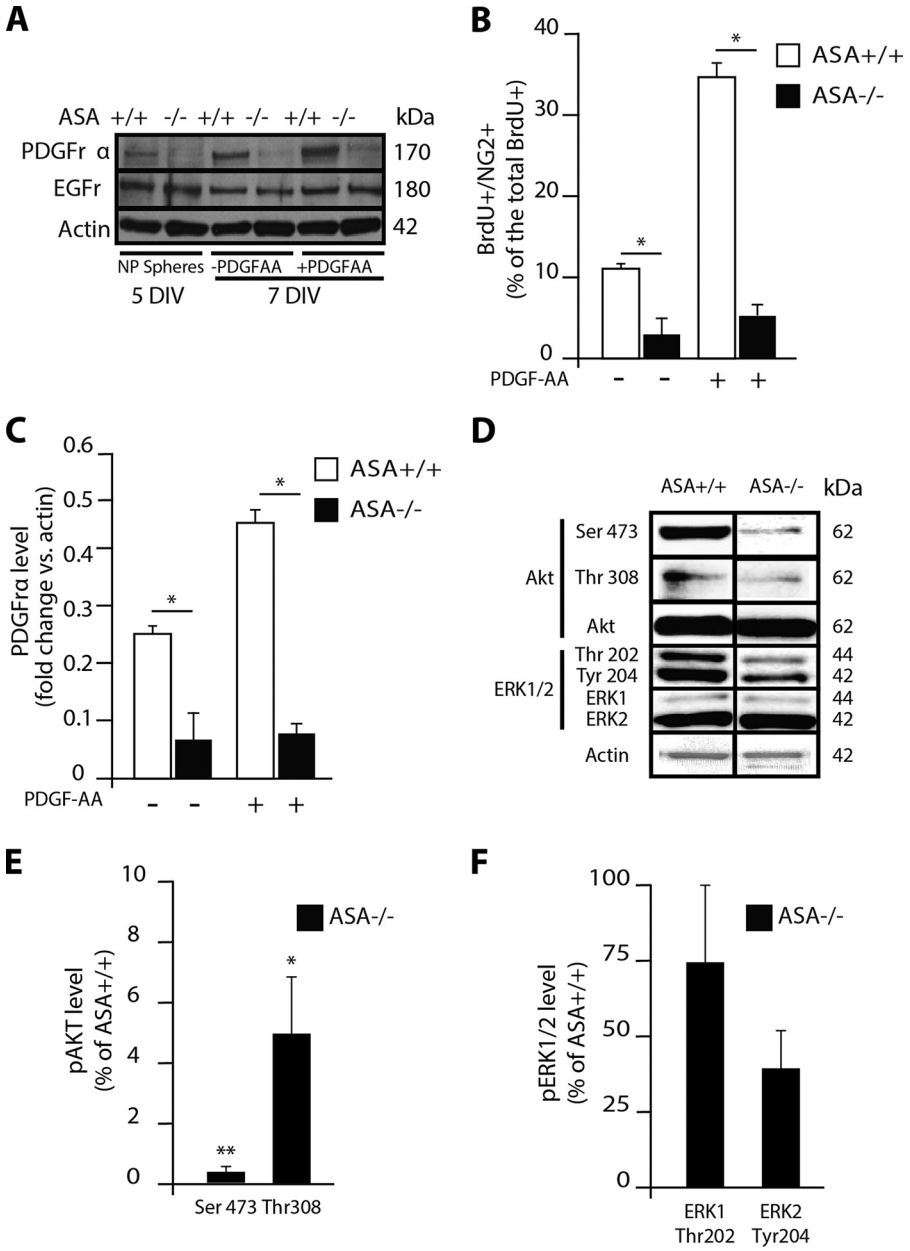

FIGURE 3. **Loss of PDGF-AA response in NPs with high sulfatide content.** *A*, immunoblotting analyses for the expression of PDGFRα, EGFR, and actin in $ASA^{+/+}$ and $ASA^{-/-}$ NPs. Analysis was performed in proliferating NPs after 5 DIV and in differentiated cells after 7 DIV in the presence or absence of 20 ng/ml PDGF-AA. PDGFRα levels were reduced in all $ASA^{-/-}$ NP conditions. *B*, $ASA^{+/+}$ and $ASA^{-/-}$ NP spheres were dissociated for differentiation and incubated with or without 20 ng/ml PDGF-AA and pulsed with BrdU. Proliferating oligodendrocyte progenitors were identified by co-localization of $NG2^+$ and $BrdU^+$ at 3 days using immunocytochemistry. $BrdU^+/NG2^+$ cells were significantly reduced in $ASA^{-/-}$ cultures (data shown as the mean ± S.E. (*error bars*); $n = 3$). *, $p < 0.05$ by Student's *t* test). *C*, semiquantification of immunodetected PDGFRα in differentiated $ASA^{-/-}$ cells. In contrast to control cells, incubation with PDGF-AA did not increase receptor levels (data shown as the mean ± S.E.; $n = 3$). $ASA^{+/+}$ *versus* $ASA^{-/-}$ (−) PDGFA, *, $p = 0.038$; $ASA^{+/+}$ *versus* $ASA^{-/-}$ (+) PDGF-AA, *, $p = 0.0025$ by Student's *t* test. *D–F*, $ASA^{+/+}$ and $ASA^{-/-}$ NPs were starved of growth factors for 3 h and exposed to PDGF-AA ligand for 30 min at 4 °C. Unbound ligand was washed off, and cells were incubated for 30 min at 37 °C. AKT phosphorylation at Thr^{308} and Ser^{473} was significantly decreased in $ASA^{-/-}$ NPs with respect to $ASA^{+/+}$ NPs. ERK1 phosphorylation at Thr^{202} and ERK2 Tyr^{204} was similar in both cell types (data shown as the mean ± S.E.; $n = 3$). *, $p \leq 0.05$; **, $p \leq 0.01$ by Student's *t* test.

PDGFRα Is Secreted via Exosomal Shedding—Receptor shedding via exosomal secretion has been shown to be an important mechanism by which cells regulate signaling with their environment (48). Exosomes are vesicles of ~20–100 nm in diameter generated through the formation of multivesicular bodies (49). Of relevance, OPCs and OLs are known to shed various proteins and lipids through exosomal secretion *in vitro* (50, 51). To determine whether PDGFRα is associated with this process, exosomes were prepared from conditioned cell culture media of $ASA^{+/+}$ and $ASA^{-/-}$ NPs. Electron microscopy examination of exosomal preparations showed that $ASA^{-/-}$ and $ASA^{+/+}$ have similar stereotypical profiles of circular vesicles with diameters ranging from ~25 to 100 nm (Fig. 4, *D* and *E*). Immunoblotting analysis of exosomal protein extracts showed significant increase in PDGFRα levels in $ASA^{-/-}$ exosomes (Fig. 4*F*), which represents about 3–4% of the reduction in PDGFRα observed in $ASA^{-/-}$ NPs. In contrast, receptor levels in $ASA^{+/+}$ exosomes were significantly lower in $ASA^{+/+}$ and

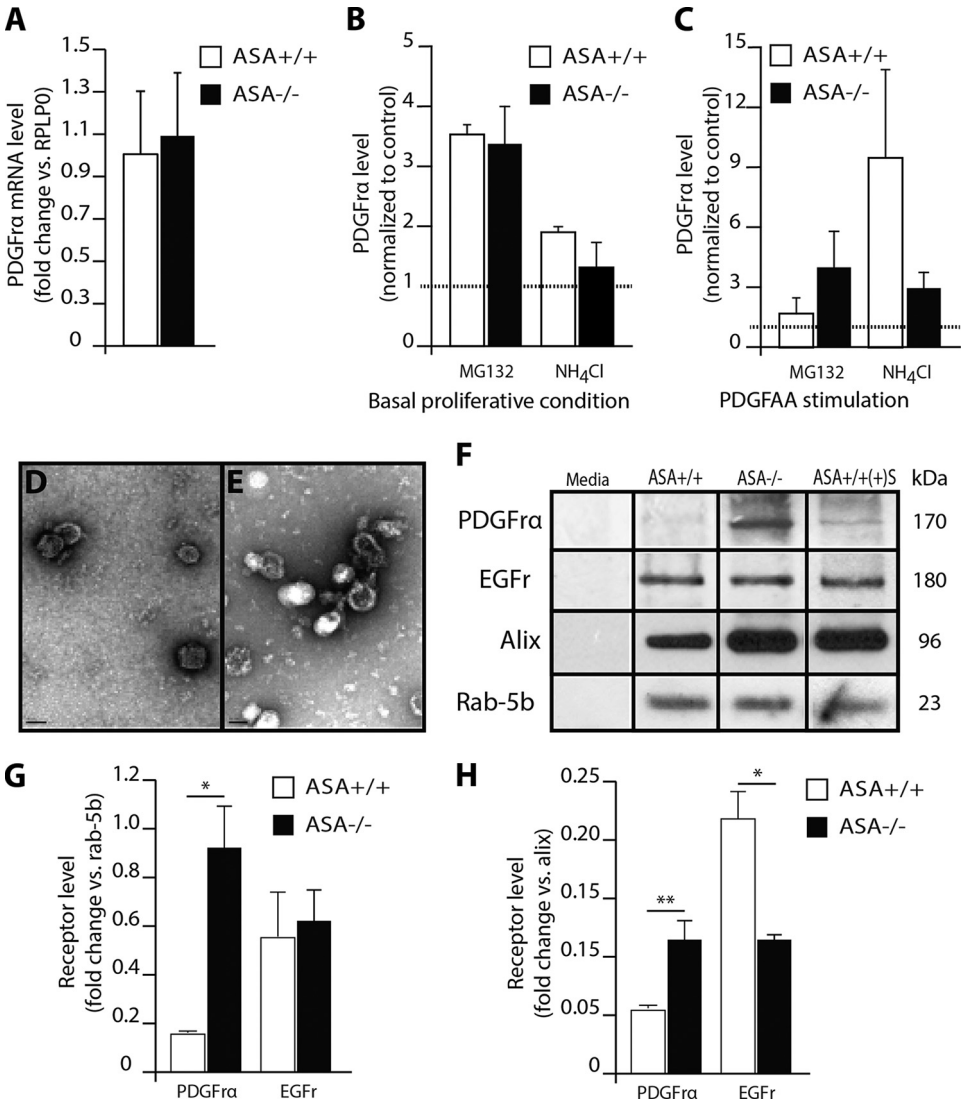

FIGURE 4. **ASA$^{-/-}$ NPs showed no differences in transcription or proteolysis but an increased exosomal secretion of PDGFRα in cells with high sulfatide content.** *A*, real-time PCR analysis of mRNA isolated from ASA$^{-/-}$ and ASA$^{+/+}$ NPs did not show significant differences in transcript levels for PDGFRα (data shown as the mean ± S.E. (*error bars*); $n = 3$; $p < 0.9$ by Student's *t* test). *B* and *C*, the effect of proteolytic inhibitor MG132 and NH4CL lysosomal inhibitor on the expression of PDFGRα showed similar recovery of receptor levels in ASA$^{+/+}$ and ASA$^{-/-}$ NPs in basal conditions and following PDGF-AA-stimulated conditions (data shown as the mean ± S.E.; $n = 3$). *D* and *E*, exosomes isolated from ASA$^{+/+}$ (*D*) and ASA$^{-/-}$ NP (*E*) culture media showed a typical vesicular shape with diameters between 30 and 100 nm. *Bars*, 50 nm. *F*, immunoblotting analysis showed the presence of higher levels of PDGFRα in exosomes released from ASA$^{-/-}$ NPs and from ASA$^{+/+}$ NP spheres treated with 10 μM sulfatides. *G* and *H*, the relative abundance of PDGFRα and of EGFR were calculated with respect to the exosomal content of Rab-5b and Alix (data shown as the mean ± S.E.; $n = 3$). *, $p \leq 0.05$ by Student's *t* test.

absent in mock medium (Fig. 4, *F–H*). Treatment of ASA$^{+/+}$ NPs with 10 μM exogenous sulfatides also led to an exosomal release of PDGFRα, although less intense than in ASA$^{-/-}$ cells, possibly due to ASA activity in ASA$^{+/+}$ cells (Fig. 4*F*). Levels of EGFR in exosomes were significantly reduced in ASA$^{-/-}$ when normalized against the exosomal housekeeping protein Alix but not against Rab-5b (Fig. 4, *G* and *H*). This may reflect compositional changes in exosomes from mutant cells.

Reduced PDGFRα in Detergent-resistant Membranes of ASA$^{-/-}$ Cells—Association of PDGFRα with DRMs is needed for its function in OPCs (33, 34). To examine whether this association was affected in ASA$^{-/-}$ cells, a Lubrol-sucrose gradient method that fractionates plasmalemma DRMs from other non-DRM membranes (lysosomes, Golgi apparatus, etc.) was used (52). Immunoblotting analyses showed a sharp reduction (~5% of the total level of receptor) of PDGFRα in DRMs (fractions 4–6) from ASA$^{-/-}$ cells (Fig. 5*A*). DRM markers flotillin 2 and caveolin 1 were also significantly reduced in mutant DRMs (Fig. 5*B*). Interestingly, exposure of ASA$^{+/+}$ cells to sulfatides led to reductions of PDGFRα in DRMs (Fig. 5*A*). The total level of cholesterol (another DRM compound) and its buoyancy were not significantly different between ASA$^{-/-}$ and ASA$^{+/+}$ (Fig. 5*C*). Sulfatides were significantly increased in DRM fractions but decreased in non-DRM fractions from ASA$^{-/-}$ cells (Fig. 5*D*). Together, these results suggest that changes in DRM composition occur in ASA$^{-/-}$ cells, contributing to a reduction of PDGFRα in the plasma membrane.

Enzyme Correction Ameliorates Gliogenic and PDGFRα Defects in ASA$^{-/-}$ Cells—To evaluate whether gliogenic and receptor deficits can be corrected in ASA$^{-/-}$ cells, enzyme replacement was done by treating ASA$^{-/-}$ cells in culture medium conditioned from ASA prepared from ASA-overex-

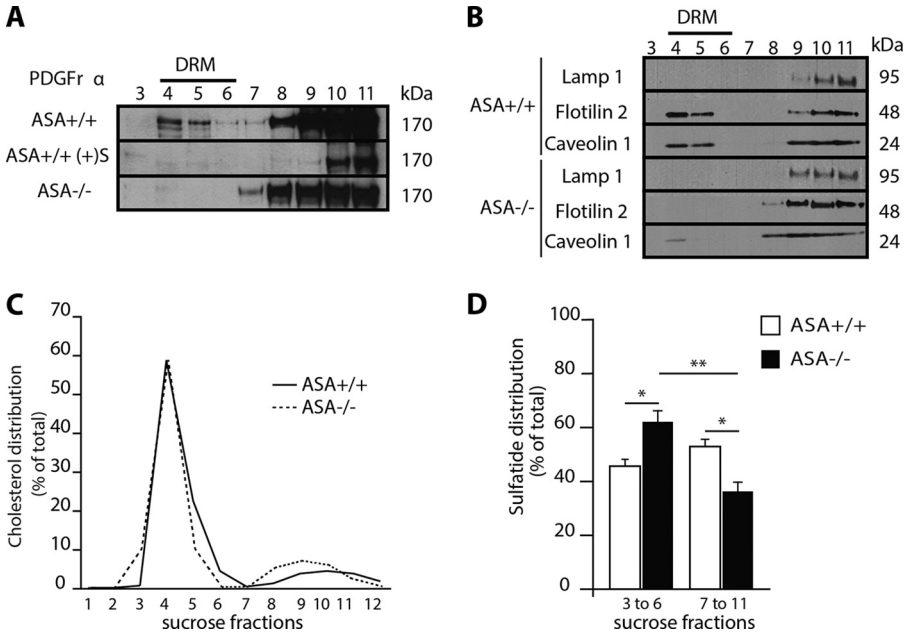

FIGURE 5. **$ASA^{-/-}$ NPs showed increased sulfatide content and a reduction in PDGFRα expression in detergent-resistant membranes.** *A* and *B*, immunoblotting for PDGFRα in DRM (fractions 4–6) and non-DRMs (fractions 7–11) showed reduced association between PDGFRα, caveolin 1, and flotillin 2 and DRMs in $ASA^{-/-}$ NPs. Flotilin 2 and caveolin 1 identified DRMs, and Lamp1 identified enriched lysosomal fraction compartments. $ASA^{+/+}$ NPs were pulsed twice with 10 μM sulfatides and showed a distribution of the PDGFRα in DRM similar to that of $ASA^{-/-}$ cells. *C*, cholesterol was measured in all sucrose fractions and showed no differences in levels between $ASA^{+/+}$ and $ASA^{-/-}$ NPs. *D*, total sulfatides were measured in DRM and non-DRM sucrose fractions of $ASA^{+/+}$ and $ASA^{-/-}$ cells by UHPLC-MS/MS. $ASA^{-/-}$ cells showed significant accumulation of sulfatides in the DRM fractions compared with $ASA^{+/+}$ cells (data shown as the mean ± S.E. (*error bars*); $n = 6$; $ASA^{+/+}$ *versus* $ASA^{-/-}$ (fractions 3–6), *, $p = 0.028$; $ASA^{+/+}$ *versus* $ASA^{-/-}$ (fractions 7–11), *, $p = 0.028$; $ASA^{-/-}$ (fractions 3–6) *versus* $ASA^{-/-}$ (fractions 7–11), **, $p = 0.01$ by analysis of variance).

pressing cells (ASACM) (36). This cross-correction experiment takes advantage of the general property of lysosomal enzymes to be taken up by cells, primarily via the endocytic mechanism involving a mannose 6-phosphate receptor (53). Cross-correction using this approach has been well established with a significant number of lysosomal enzymes, including ASA (54). $ASA^{-/-}$ NP spheres were incubated with 5, 10, or 25% ASACM before analysis. Immunocytochemical detection of ASA protein by confocal microscopy showed intracellular presence of ASA in corrected $ASA^{-/-}$ cells (Fig. 6*A*). ASA enzyme activity was substantially recovered (data not shown). Although sulfatide content was not normalized, there was a significant recovery of the normal ratio of long *versus* short fatty acid sulfatides in cells cultured with 25% ASACM (Fig. 6*B*).

Levels of PDGFRα were significantly normalized in corrected $ASA^{-/-}$ cells (Fig. 6*C*). Recovery of PDGFRα led to significant relocalization of the receptor in DRM fractions and less exosomal shedding (Fig. 6*D*). A significant recovery of AKT phosphorylation at serine residue 473 was observed but not in ERK1/2 phosphorylation (Fig. 6, *E* and *F*). Upon differentiation, production of $O4^+$ OLs from corrected $ASA^{-/-}$ cells was significantly normalized (Fig. 6*G*).

Exosomal Secretion of PDGFRα Occurs in Oligodendroglial Cells—Our experiments of exosomal shedding are relevant because this may be a regulatory mechanism used by OLs to locally and rapidly control levels of receptor available at the cell surface. To study this process in more detail, we measured receptor levels in exosomes isolated from primary glial cultures, CG4 cells (central glial-4 cells) and in the murine cortex. First, mixed glial cultures were prepared from newborn $ASA^{+/+}$ and $ASA^{-/-}$ pups and maintained for 7, 14, and 21 DIV, to enrich immature $A2B5^+/NG2^+$ OPCs (7 DIV) or intermediate $O4^+$, $O1^+$, and mature MBP^+ OLs (14 and 21 DIV), respectively (28, 55). Quality control of OL differentiation in these conditions was confirmed by Western blot analysis of MBP expression (Fig. 7*A*). Whereas $ASA^{+/+}$ glial cultures showed the expected increase of MBP during culture differentiation, OL differentiation was markedly reduced in $ASA^{-/-}$ glial cultures (Fig. 7*A*). Exosomes were isolated from conditioned medium at each time point and analyzed for PDGFRα content by immunoblotting. PDGFRα was found in low but significant levels in exosomes from $ASA^{+/+}$ glia (Fig. 7, *B* and *C*). As expected, PDGFRα was increased in exosomes from $ASA^{-/-}$ glia (Fig. 7, *B* and *C*). A similar analysis was done with conditioned medium from cultures of oligodendroglial CG4 cells. Cells were grown in proliferating conditions for 5 DIV before analysis of exosomes. Immunodetectable levels of PDGFRα were present in the conditioned medium (Fig. 7*D*), indicating that this process occurs in OPCs independently of astrocytes being present.

Finally, we examined the extent to which exosomal shedding of PDGFRα occurs during myelination in the mouse brain. For this, we adapted a previously described technique (34). Transmission electron microscopy imaging confirmed the exosomal ultrastructure of these preparations from $ASA^{+/+}$ and $ASA^{-/-}$ brain material (Fig. 7*E*). Subsequent immunoblotting analysis showed the presence of PDGFRα (Fig. 7*F*) in brain exosomes from both genotypes. Exosomal shedding of PLP was used as a quality control for our experiments (Fig. 7*G*). This analysis showed a peak of the receptor in exosomes isolated from the cortex of P14 $ASA^{+/+}$ brain (Fig. 7*F*), a trend that was also observed in primary glial cell cultures (Fig. 7*C*). In contrast, PDGFRα levels were higher in exosomes from the $ASA^{-/-}$ cor-

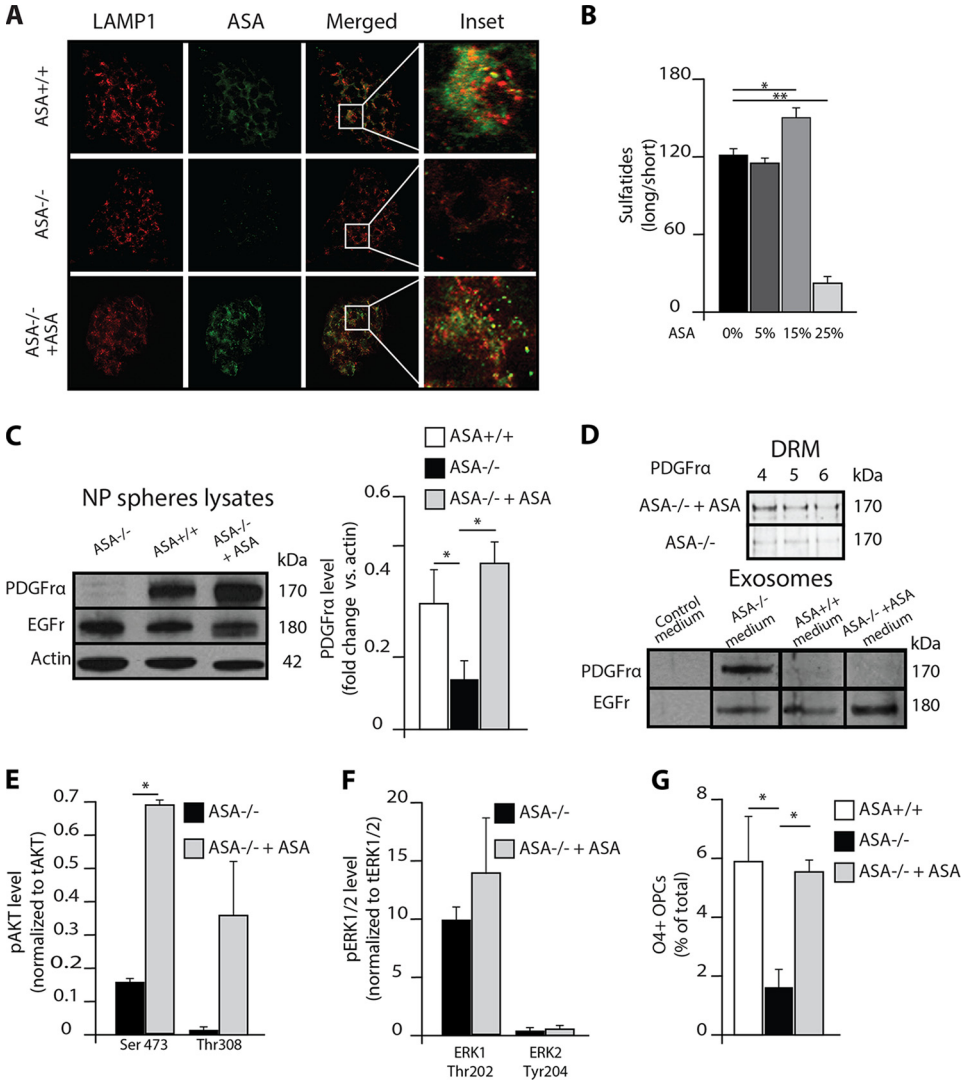

FIGURE 6. **ASA-corrected ASA$^{-/-}$ NPs and recovery of PDGFRα.** *A*, confocal immunocytochemical analysis of ASA (in *green*) showed its association with Lamp1^{+} lysosomes (in *red*) in ASA$^{+/+}$ NPs and the absence of ASA expression in ASA−/− NPs. ASA−/− cells treated with 25% ASA conditioned medium exhibited association with lysosomes (*yellow*). *B*, ASA-corrected ASA−/− NPs showed a significant reduction in the ratio of long (C24:0 and C24:1) *versus* short (C16:0 and C18:0) fatty acid isoforms in treatments with 25% conditioned medium (ASACM) but not with 5 or 15% ASACM ($n = 3$). *, $p \leq 0.05$; **, $p \leq 0.01$ by analysis of variance. *C*, immunoblotting analysis of ASA-corrected ASA$^{-/-}$ NPs showed a normalization of PDGFRα levels in NPs cell lysates. *D*, PDGFRα protein expression levels also recovered in DRMs and decreased in exosomes from enzymatically corrected ASA$^{-/-}$ NPs. *E*, AKT Ser^{473} but not Thr^{308} showed a significant decrease in phosphorylation in ASA$^{-/-}$ NPs. *F*, ERK1 phosphorylation at Thr^{202}, ERK2 at Tyr^{204} was similar in both cell types (data shown as the mean ± S.E.; $n = 3$). *, $p < 0.05$ by Student's *t* test. *G*, enzymatically corrected ASA$^{-/-}$ NPs generated significantly more O4^{+} OLs than untreated ASA$^{-/-}$ NPs 7 days after differentiation (data shown as the mean ± S.E.; $n = 3$). *, $p \leq 0.05$ by Student's *t* test.

tex. Altogether, these results provide evidence that PDGFRα is exosomally secreted *in vivo* during the peak of myelination. Contextual changes, such as sulfatide accumulation, that alter this process may be relevant to understand possible defects in myelination in the brains of metachromatic leukodystrophy patients and in other demyelinating conditions.

DISCUSSION

This study provides insight into the interaction between sulfatides and PDGFRα activity in NPs. Experimental conditions that genetically or exogenously lead to increased sulfatide content revealed 1) defects in the association of PDGFRα with DRMs, 2) impaired translation of PDGF-AA signaling via repression of PDGFRα/AKT activation, 3) increased shedding of PDGFRα via exosomes, and 4) decreased formation of NG2^{+} OPCs and O4^{+} OLs.

Various studies have shown that OL differentiation could either be promoted by a deficient synthesis of sulfatides (56, 57) or inhibited by anti-sulfatide antibodies (58, 59), suggesting that sulfatides negatively regulate OL differentiation (20, 21). However, the mechanism of this repression has remained unaddressed. Our results using ASA$^{-/-}$ NPs with intrinsically high levels of sulfatides support the idea that these lipids are associated with reduced capacity to generate OLs, in line with previous *in vivo* analyses (60).

Although sulfatides are major components of mature myelin, they are synthesized during neural development in two distinct waves, first of short and then long fatty acid sulfatides, coinciding with the appearance of immature OPCs and more differentiated OLs, respectively (61). The physiological relevance of this change remains unclear. Recently published studies from our laboratory showed that short (C16:0 and C18:0) and long

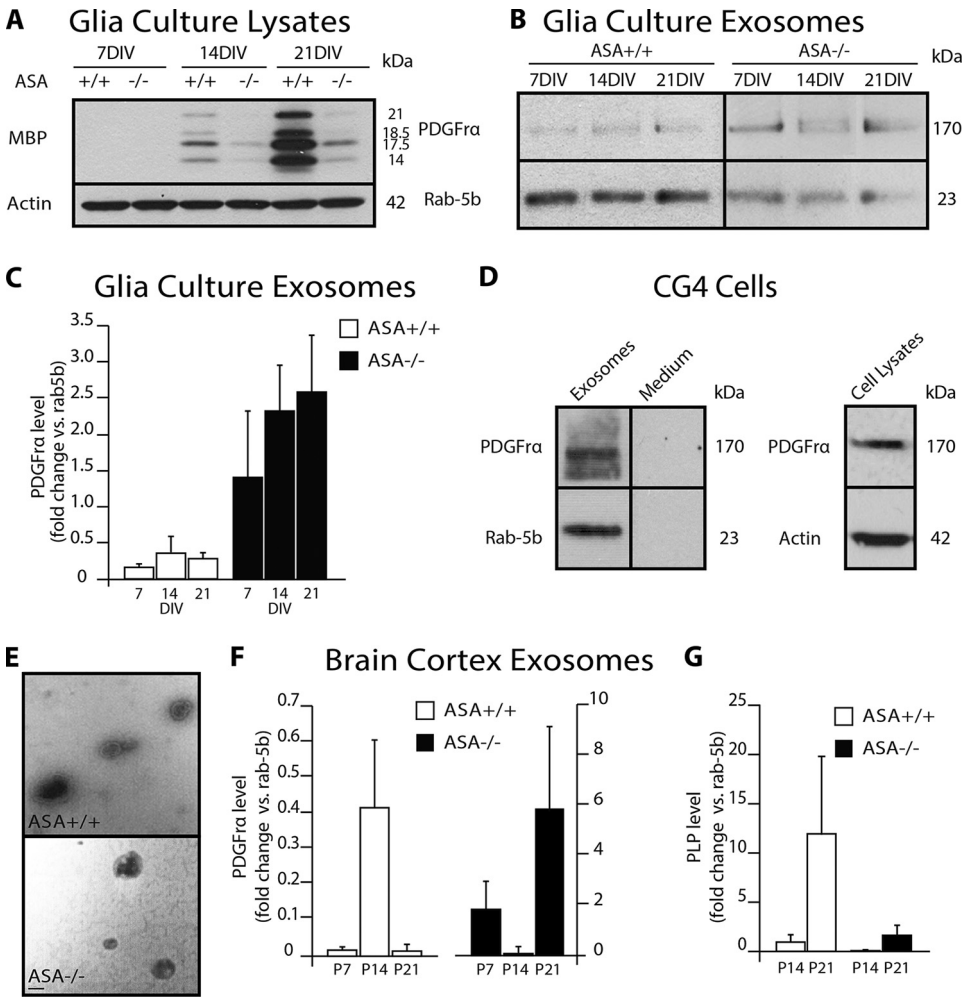

FIGURE 7. **Exosomal shedding of PDGFRα is a naturally occurring event in OLs and during myelination.** *A*, immunoblotting analysis of mouse primary glial cultures at 7, 14, and 21 days *in vitro* showed a delay in MBP expression in $ASA^{-/-}$ cells with respect to matching $ASA^{+/+}$ cultures. $ASA^{+/+}$ cells showed high levels of MBP expression at 21 days in culture. *B*, exosomes were isolated from 7-, 14-, and 21-day-old $ASA^{+/+}$ and $ASA^{-/-}$ glial culture-conditioned media. Immunoblotting analysis showed the presence of PDGFRα in exosomes from cells with normal or increased sulfatide content. Rab-5b was used as an exosomal marker. *C*, exosomal secretion of PDGFRα is a naturally occurring event in cells with normal sulfatide content ($ASA^{+/+}$). Release of the receptor continuously increased as $ASA^{-/-}$ glial cultures matured *in vitro* (data shown as the mean ± S.D. (*error bars*); $n = 3$). *D*, immunoblotting analysis of cell lysates and exosomes from CG4 cells grown in proliferative conditions showed that PDGFRα is secreted. *E*, electron microscopy of exosomes isolated from cortices of $ASA^{+/+}$ and $ASA^{-/-}$ cortices. *Bars*, 100 nm. *F* and *G*, PDGFRα and PLP expression was determined by semiquantitative immunoblotting in exosomes isolated from cortices of postnatal day (*P*) 14 and 21 mice. Exosomal secretion of PDGFRα in both $ASA^{+/+}$ and $ASA^{-/-}$ cortices increased at postnatal day 14 and also at postnatal days 7 and 21 in $ASA^{-/-}$. The level of PLP secretion was reduced in the $ASA^{-/-}$ cortex at both ages compared with $ASA^{+/+}$ (data shown as the mean ± S.E.; $n = 3$).

(C24:0 and C24:1) fatty acid sulfatides are components of DRMs isolated from $ASA^{+/+}$ and $ASA^{-/-}$ brains and that their relative abundance is developmentally regulated (32). We propose that variations in short/long sulfatide isoforms may affect the fluidity of DRMs and induce changes in PDGFRα signaling (60, 62, 63). Our findings of a significant reduction of the ratio of long *versus* short fatty acid sulfatides associated with a normalization of the PDGFRα levels and AKT phosphorylation in ASA-corrected NPs support this hypothesis.

PDGFRα regulates the proliferation, survival, and differentiation of OPCs and OLs (10, 11, 39, 64, 65), a function that is dependent on its association with DRMs (16). Interestingly, PDGFRα membrane localization responds to changes in sphingolipid content (66). For example, ganglioside GM1 induced the relocation of PDGFRα to non-DRM/caveolar membranes, inhibiting PDGFRα signaling (67). Our study identified sulfatides as another group of sphingolipids with the capacity to reduce the association of the PDGFRα with DRMs and, consequently, impair the sensitivity of $ASA^{-/-}$ NPs to PDGF-AA. This defect did not appear to be caused by a reduction in gene transcription, increased degradation, or activation of cellular stress responses to the accumulation of sulfatides but rather to the impaired activity of the PDGFRα/AKT pathway. This most likely stems from lowered association of the receptor with DRMs in $ASA^{-/-}$ NPs. Interestingly, the survival/expansion of OPC mediated by PDGF-AA involves the activation of AKT through phosphorylation of residues Thr^{308} and Ser^{473} (68, 69). Our results demonstrate that in the presence of high levels of sulfatides, the relocalization of PDGFRα to non-DRM domains and phosphorylation of Thr^{308} and Ser^{473} of AKT are severely compromised. These findings further underline the importance of DRM integrity in AKT signaling activation (70, 71). Although the molecular mechanism by which sulfatides reduce the association of the receptor in DRMs is unclear, the involve-

ment of sulfatides in this process is demonstrated by its normalization observed after correction of the ASA deficiency and the reduction in the ratio of long and short sulfatides in treated $ASA^{-/-}$ NPs. Further experimentation is under way to study the molecular mechanism mediating this effect.

Our study identifies a novel cellular mechanism contributing to the regulation of the PDGFRα in NPs via exosomal shedding. The amount of receptor secreted by exosomes corresponds to about 3–4% of the PDGFRα reduction in $ASA^{-/-}$ NPs, which is similar to the fraction of receptor associated with DRM. These findings suggest that the fraction of receptor associated with DRM is subjected to exosome control. Low levels of PDGFRα in DRMs may be sufficient to interfere with critical survival/proliferation signaling in OPCs. This would weaken the capacity of the $ASA^{-/-}$ cultures to generate normal numbers of OPCs and OLs and explain the reduction on PDGFRα levels.

Exosomes are intralumenal vesicles contained in multivesicular bodies playing important roles in cell-cell communication (72–75), and their shedding is a physiological relevant process. For example, the transferrin receptor and the myelin protein PLP undergo exosomal secretion during differentiation of erythrocytes and OLs, respectively (26, 51, 76). Sphingolipids contribute to regulating the formation of exosomes (77, 78), and cholesterol and ceramides promote exosome secretion (76, 79–81). Our experiments suggest a role for sulfatides in exosomal biogenesis. Intrinsic increases in sulfatides, such as in $ASA^{-/-}$ NPs, and, to a lesser extent, acute exposure to exogenous sulfatides promoted the shedding of PDGFRα. Exosomal shedding of PDGFRα in glial cells has not been reported previously, but this secretory mechanism may be a relevant physiological process by which OPCs rapidly and locally regulate the concentration of receptor. In turn, this may have an immediate impact on the receptor-mediated responses to proliferation, survival, and/or differentiation.

How PDGFRα translocates to exosomes and is targeted for removal is still unclear. We hypothesize this process could involve changes in lipid-protein composition in membrane domains where the receptor is assembled. The changes in long *versus* short fatty acid sulfatides observed in DRMs in our study appear to support this. At this moment, excluding the EGFR, the possibility that other receptors are fated to exosomal secretion cannot be ruled out. Confocal microscopy studies suggested co-localization of PDGFRα with sulfatides in $ASA^{+/+}$ and to a lesser extent in $ASA^{-/-}$ NPs (data not shown). There is evidence that sulfatides are components of exosomal membranes (82). However, exosomes isolated from NPs appeared to contain little if any sulfatide (data not shown). This last observation suggests that PDGFRα and sulfatides might use different intracellular vesicular trafficking compartments. The reduction of PDGFRα from DRMs upon increased concentrations of sulfatides supports this conclusion.

In vivo studies in the $ASA^{+/+}$ cortex showed an increase in exosomal secretion of PDGFRα before the peak of myelination. These results provide further evidence that exosomal regulation of PDGFRα might be part of a larger regulatory program involved in myelination. Sulfatides may contribute to the control of the local amount of PDGFRα available in the OPC cell body to respond effectively to PDGF-AA during myelination. *In vivo*, exosomal shedding may involve other mechanisms, including axonal signals, nerve conduction, and astrocytic and microglial signals (83–88). In this scenario, one of the events occurring when OPCs stop dividing and start myelination is the production of large quantities of sulfatides to cope with the production of the myelin membrane. Such conditions may activate the exosomal loss of PDGFRα from OPCs to coordinate its postmitotic cycle and myelinating program. Studies by Trajkovic *et al.* (50) and Bakhti *et al.* (51) demonstrating a fundamental role of endosomes and exosomes during OL maturation and myelination appear to support this model. Whether this mechanism is also relevant in tethering OL numbers during CNS development and remyelination is currently unknown.

In the context of the ASA deficiency, our study provides an initial understanding of how ASA deficiency and sulfatides may contribute to demyelination and remyelination defects in the human lysosomal storage disease metachromatic leukodystrophy (60). Our observations may also be extrapolated to other demyelinating diseases, such as multiple sclerosis, where demyelination could lead to the availability of myelin debris, transforming myelin-derived sulfatides into environmental toxins (31, 89–91) that may impair remyelination. In this regard, other myelin components, such as myelin-associated glycoprotein, myelin oligodendrocyte glycoprotein, and Nogo A, are known to exert inhibitory functions, decreasing the regenerative capacity of the brain (92–94).

Our work may also extend to non-neural situations. For example, sulfatides are also expressed in non-nervous tissues, such as renal and pancreatic tissues, where they have been described as participating in the secretion of insulin (95–97), and they are elevated in a wide range of cancers, where they are thought to participate in metastasis (98–100). In some of these diseases, sulfatides may contribute to pathology by altering the regulation of local signals via changes in DRMs and/or exosomal secretion. Because sulfatides comprise a heterogeneous population of lipids, future studies will need to determine the physiological role of the different sulfatide isoforms.

Acknowledgments—We thank Zhiyuan Sun for technical assistance in mass spectrometry and Dr. Gerardo Morfini for relevant experimental discussions.

Note Added in Proof—Refs. 8, 9, 13, 18, 19, 23, 24, 39–41, 45–47, 53, and 64 were not correct in the version of this article that was published on January 20, 2015 as a Paper in Press. The correct references are now cited.

REFERENCES

1. Pringle, N. P., Yu, W. P., Guthrie, S., Roelink, H., Lumsden, A., Peterson, A. C., and Richardson, W. D. (1996) Determination of neuroepithelial cell fate: induction of the oligodendrocyte lineage by ventral midline cells and sonic hedgehog. *Dev. Biol.* **177,** 30–42
2. Richardson, W. D., Pringle, N. P., Yu, W. P., and Hall, A. C. (1997) Origins of spinal cord oligodendrocytes: possible developmental and evolutionary relationships with motor neurons. *Dev. Neurosci.* **19,** 58–68
3. Orentas, D. M., Hayes, J. E., Dyer, K. L., and Miller, R. H. (1999) Sonic hedgehog signaling is required during the appearance of spinal cord oligodendrocyte precursors. *Development* **126,** 2419–2429
4. Alberta, J. A., Park, S. K., Mora, J., Yuk, D., Pawlitzky, I., Iannarelli, P., Vartanian, T., Stiles, C. D., and Rowitch, D. H. (2001) Sonic hedgehog is

required during an early phase of oligodendrocyte development in mammalian brain. *Mol. Cell Neurosci.* **18,** 434–441
5. Warf, B. C., Fok-Seang, J., and Miller, R. H. (1991) Evidence for the ventral origin of oligodendrocyte precursors in the rat spinal cord. *J. Neurosci.* **11,** 2477–2488
6. Barres, B. A., Lazar, M. A., and Raff, M. C. (1994) A novel role for thyroid hormone, glucocorticoids and retinoic acid in timing oligodendrocyte development. *Development* **120,** 1097–1108
7. Chong, S. Y., and Chan, J. R. (2010) Tapping into the glial reservoir: cells committed to remaining uncommitted. *J. Cell Biol.* **188,** 305–312
8. Raff, M. C., Lillien, L. E., Richardson, W. D., Burne, J. F., and Noble, M. D. (1988) Platelet-derived growth factor from astrocytes drives the clock that times oligodendrocyte development in culture. *Nature* **333,** 562–565
9. Richardson, W. D., Pringle, N., Mosley, M. J., Westermark, B., and Dubois-Dalcq, M. (1988) A role for platelet-derived growth factor in normal gliogenesis in the central nervous system. *Cell* **53,** 309–319
10. Noble, M., Murray, K., Stroobant, P., Waterfield, M. D., and Riddle, P. (1988) Platelet-derived growth factor promotes division and motility and inhibits premature differentiation of the oligodendrocyte/type-2 astrocyte progenitor cell. *Nature* **333,** 560–562
11. Chojnacki, A., Mak, G., and Weiss, S. (2011) PDGFRα expression distinguishes GFAP-expressing neural stem cells from PDGF-responsive neural precursors in the adult periventricular area. *J. Neurosci.* **31,** 9503–9512
12. Hall, A., Giese, N. A., and Richardson, W. D. (1996) Spinal cord oligodendrocytes develop from ventrally derived progenitor cells that express PDGF α-receptors. *Development* **122,** 4085–4094
13. Pringle, N. P., Mudhar, H. S., Collarini, E. J., and Richardson, W. D. (1992) PDGF receptors in the CNS: during late neurogenesis, expression of PDGF alpha receptors appears to be restricted to glial cells of the oligodendrocyte lineage. *Development* **115,** 535–551
14. Fruttiger, M., Karlsson, L., Hall, A. C., Abramsson, A., Calver, A. R., Boström, H., Willetts, K., Bertold, C. H., Heath, J. K., Betsholtz, C., and Richardson, W. D. (1999) Defective oligodendrocyte development and severe hypomyelination in PDGF-A knockout mice. *Development* **126,** 457–467
15. Baron, W., Shattil, S. J., and ffrench-Constant, C. (2002) The oligodendrocyte precursor mitogen PDGF stimulates proliferation by activation of α(v)β3 integrins. *EMBO J.* **21,** 1957–1966
16. Baron, W., Decker, L., Colognato, H., and ffrench-Constant, C. (2003) Regulation of integrin growth factor interactions in oligodendrocytes by lipid raft microdomains. *Curr. Biol.* **13,** 151–155
17. Decker, L., Baron, W., and Ffrench-Constant, C. (2004) Lipid rafts: microenvironments for integrin-growth factor interactions in neural development. *Biochem. Soc. Trans.* **32,** 426–430
18. Givogri, M. I., Bottai, D., Zhu, H. L., Fasano, S., Lamorte, G., Brambilla, R., Vescovi, A., Wrabetz, L., and Bongarzone, E. (2008) Multipotential neural precursors transplanted into the metachromatic leukodystrophy brain fail to generate oligodendrocytes but contribute to limit brain dysfunction. *Dev. Neurosci.* **30,** 340–357
19. Bosio, A., Binczek, E., Haupt, W. F., and Stoffel, W. (1998) Composition and biophysical properties of myelin lipid define the neurological defects in galactocerebroside- and sulfatide-deficient mice. *J. Neurochem.* **70,** 308–315
20. Bansal, R., Winkler, S., and Bheddah, S. (1999) Negative regulation of oligodendrocyte differentiation by galactosphingolipids. *J. Neurosci.* **19,** 7913–7924
21. Hirahara, Y., Bansal, R., Honke, K., Ikenaka, K., and Wada, Y. (2004) Sulfatide is a negative regulator of oligodendrocyte differentiation: development in sulfatide-null mice. *Glia* **45,** 269–277
22. Simons, K., and Ikonen, E. (1997) Functional rafts in cell membranes. *Nature* **387,** 569–572
23. Thompson, T. E., and Tillack, T. W. (1985) Organization of glycosphingolipids in bilayers and plasma membranes of mammalian cells. *Annu. Rev. Biophys. Biophys. Chem.* **14,** 361–386
24. White, A. B., Galbiati, F., Givogri, M. I., Lopez Rosas, A., Qiu, X., van Breemen, R., and Bongarzone, E. R. (2011) Persistence of psychosine in brain lipid rafts is a limiting factor in the therapeutic recovery of a mouse model for Krabbe disease. *J. Neurosci. Res.* **89,** 352–364
25. Carayon, K., Chaoui, K., Ronzier, E., Lazar, I., Bertrand-Michel, J., Roques, V., Balor, S., Terce, F., Lopez, A., Salomé, L., and Joly, E. (2011) Proteolipidic composition of exosomes changes during reticulocyte maturation. *J. Biol. Chem.* **286,** 34426–34439
26. de Gassart, A., Geminard, C., Fevrier, B., Raposo, G., and Vidal, M. (2003) Lipid raft-associated protein sorting in exosomes. *Blood* **102,** 4336–4344
27. Givogri, M. I., de Planell, M., Galbiati, F., Superchi, D., Gritti, A., Vescovi, A., de Vellis, J., and Bongarzone, E. R. (2006) Notch signaling in astrocytes and neuroblasts of the adult subventricular zone in health and after cortical injury. *Dev. Neurosci.* **28,** 81–91
28. Givogri, M. I., Bongarzone, E. R., Schonmann, V., and Campagnoni, A. T. (2001) Expression and regulation of golli products of myelin basic protein gene during *in vitro* development of oligodendrocytes. *J. Neurosci. Res.* **66,** 679–690
29. Louis, J. C., Muir, D., and Varon, S. (1992) Autocrine inhibition of mitotic activity in cultured oligodendrocyte-type-2 astrocyte (O-2A) precursor cells. *Glia* **6,** 30–38
30. Folch, J., Lees, M., and Sloane Stanley, G. H. (1957) A simple method for the isolation and purification of total lipides from animal tissues. *J. Biol. Chem.* **226,** 497–509
31. Moyano, A. L., Pituch, K., Li, G., van Breemen, R., Mansson, J. E., and Givogri, M. I. (2013) Levels of plasma sulfatides C18:0 and C24:1 correlate with disease status in relapsing-remitting multiple sclerosis. *J. Neurochem.* **127,** 600–604
32. Moyano, A. L., Li, G., Lopez-Rosas, A., Månsson, J. E., van Breemen, R. B., and Givogri, M. I. (2014) Distribution of C16:0, C18:0, C24:1, and C24:0 sulfatides in central nervous system lipid rafts by quantitative ultra-high-pressure liquid chromatography tandem mass spectrometry. *Anal. Biochem.* **467,** 31–39
33. Bodennec, J., Brichon, G., Zwingelstein, G., and Portoukalian, J. (2000) Purification of sphingolipid classes by solid-phase extraction with aminopropyl and weak cation exchanger cartridges. *Methods Enzymol.* **312,** 101–114
34. Perez-Gonzalez, R., Gauthier, S. A., Kumar, A., and Levy, E. (2012) The exosome secretory pathway transports amyloid precursor protein carboxyl-terminal fragments from the cell into the brain extracellular space. *J. Biol. Chem.* **287,** 43108–43115
35. Thery, C., Amigorena, S., Raposo, G., and Clayton, A. (2006) Isolation and characterization of exosomes from cell culture supernatants and biological fluids. *Curr. Protoc. Cell Biol.* 10.1002/0471143030.cb0322s30
36. Luca, T., Givogri, M. I., Perani, L., Galbiati, F., Follenzi, A., Naldini, L., and Bongarzone, E. R. (2005) Axons mediate the distribution of arylsulfatase A within the mouse hippocampus upon gene delivery. *Mol. Ther.* **12,** 669–679
37. Porter, M. T., Fluharty, A. L., and Kihara, H. (1969) Metachromatic leukodystrophy: arylsulfatase-A deficiency in skin fibroblast cultures. *Proc. Natl. Acad. Sci. U.S.A.* **62,** 887–891
38. Yaghootfam, A., Gieselmann, V., and Eckhardt, M. (2005) Delay of myelin formation in arylsulphatase A-deficient mice. *Eur. J. Neurosci.* **21,** 711–720
39. Richardson, W. D., Pringle, N., Mosley, M. J., Westermark, B., and Dubois-Dalcq, M. (1988) A role for platelet-derived growth factor in normal gliogenesis in the central nervous system. *Cell* **53,** 309–319
40. McKinnon, R. D., Matsui, T., Aranda, M., and Dubois-Dalcq, M. (1991) A role for fibroblast growth factor in oligodendrocyte development. *Ann. N. Y. Acad. Sci.* **638,** 378–386
41. Butt, A. M., Hornby, M. F., Ibrahim, M., Kirvell, S., Graham, A., and Berry, M. (1997) PDGF-alpha receptor and myelin basic protein mRNAs are not coexpressed by oligodendrocytes *in vivo*: a double *in situ* hybridization study in the anterior medullary velum of the neonatal rat. *Mol. Cell Neurosci.* **8,** 311–322
42. Bhat, N. R., and Zhang, P. (1996) Activation of mitogen-activated protein kinases in oligodendrocytes. *J. Neurochem.* **66,** 1986–1994
43. Baron, W., Metz, B., Bansal, R., Hoekstra, D., and de Vries, H. (2000) PDGF and FGF-2 signaling in oligodendrocyte progenitor cells: regula-

tion of proliferation and differentiation by multiple intracellular signaling pathways. *Mol. Cell Neurosci.* **15,** 314–329
44. Klinghoffer, R. A., Hamilton, T. G., Hoch, R., and Soriano, P. (2002) An allelic series at the PDGFαR locus indicates unequal contributions of distinct signaling pathways during development. *Dev. Cell* **2,** 103–113
45. Gonzalez-Gaitan, M. (2008) The garden of forking paths: recycling, signaling, and degradation. *Dev. Cell* **15,** 172–174
46. Acconcia, F., Sigismund, S., and Polo, S. (2009) Ubiquitin in trafficking: the network at work. *Exp. Cell Res.* **315,** 1610–1618
47. Gonnord, P., Blouin, C. M., and Lamaze, C. (2012) Membrane trafficking and signaling: two sides of the same coin. *Semin. Cell Dev. Biol.* **23,** 154–164
48. Blanc, L., and Vidal, M. (2010) Reticulocyte membrane remodeling: contribution of the exosome pathway. *Curr. Opin. Hematol* **17,** 177–183
49. Lai, C. P., and Breakefield, X. O. (2012) Role of exosomes/microvesicles in the nervous system and use in emerging therapies. *Front. Physiol.* **3,** 228
50. Trajkovic, K., Dhaunchak, A. S., Goncalves, J. T., Wenzel, D., Schneider, A., Bunt, G., Nave, K. A., and Simons, M. (2006) Neuron to glia signaling triggers myelin membrane exocytosis from endosomal storage sites. *J. Cell Biol.* **172,** 937–948
51. Bakhti, M., Winter, C., and Simons, M. (2011) Inhibition of myelin membrane sheath formation by oligodendrocyte-derived exosome-like vesicles. *J. Biol. Chem.* **286,** 787–796
52. White, A. B., Givogri, M. I., Lopez-Rosas, A., Cao, H., van Breemen, R., Thinakaran, G., and Bongarzone, E. R. (2009) Psychosine accumulates in membrane microdomains in the brain of Krabbe patients, disrupting the raft architecture. *J. Neurosci.* **29,** 6068–6077
53. Du, H., Levine, M., Ganesa, C., Witte, D. P., Cole, E. S., and Grabowski, G. A. (2005) The role of mannosylated enzyme and the mannose receptor in enzyme replacement therapy. *Am. J. Hum. Genet.* **77,** 1061–1074
54. Givogri, M. I., Galbiati, F., Fasano, S., Amadio, S., Perani, L., Superchi, D., Morana, P., Del Carro, U., Marchesini, S., Brambilla, R., Wrabetz, L., and Bongarzone, E. (2006) Oligodendroglial progenitor cell therapy limits central neurological deficits in mice with metachromatic leukodystrophy. *J. Neurosci.* **26,** 3109–3119
55. McCarthy, K. D., and de Vellis, J. (1980) Preparation of separate astroglial and oligodendroglial cell cultures from rat cerebral tissue. *J. Cell Biol.* **85,** 890–902
56. Bosio, A., Binczek, E., and Stoffel, W. (1996) Functional breakdown of the lipid bilayer of the myelin membrane in central and peripheral nervous system by disrupted galactocerebroside synthesis. *Proc. Natl. Acad. Sci. U.S.A.* **93,** 13280–13285
57. Coetzee, T., Fujita, N., Dupree, J., Shi, R., Blight, A., Suzuki, K., Suzuki, K., and Popko, B. (1996) Myelination in the absence of galactocerebroside and sulfatide: normal structure with abnormal function and regional instability. *Cell* **86,** 209–219
58. Dyer, C. A., and Benjamins, J. A. (1988) Antibody to galactocerebroside alters organization of oligodendroglial membrane sheets in culture. *J. Neurosci.* **8,** 4307–4318
59. Bansal, R., and Pfeiffer, S. E. (1989) Reversible inhibition of oligodendrocyte progenitor differentiation by a monoclonal antibody against surface galactolipids. *Proc. Natl. Acad. Sci. U.S.A.* **86,** 6181–6185
60. Gieselmann, V., Franken, S., Klein, D., Mansson, J. E., Sandhoff, R., Lullmann Rauch, R., Hartmann, D., Saravanan, V. P., De Deyn, P. P., D'Hooge, R., Van Der Linden, A. M., and Schaeren-Wiemers, N. (2003) Metachromatic leukodystrophy: consequences of sulphatide accumulation. *Acta Paediatr. Suppl.* **92,** 74–79; discussion 45
61. Burkart, T., Hofmann, K., Siegrist, H. P., Herschkowitz, N. N., and Wiesmann, U. N. (1981) Quantitative measurement of *in vivo* sulfatide metabolism during development of the mouse brain: evidence for a large rapidly degradable sulfatide pool. *Dev. Biol.* **83,** 42–48
62. Helms, J. B., and Zurzolo, C. (2004) Lipids as targeting signals: lipid rafts and intracellular trafficking. *Traffic* **5,** 247–254
63. Simons, K., and Gerl, M. J. (2010) Revitalizing membrane rafts: new tools and insights. *Nat. Rev. Mol. Cell Biol.* **11,** 688–699
64. Collarini, E. J., Pringle, N., Mudhar, H., Stevens, G., Kuhn, R., Monuki, E. S., Lemke, G., and Richardson, W. D. (1991) Growth factors and transcription factors in oligodendrocyte development. *J. Cell Sci. Suppl.* **15,** 117–123
65. Hart, I. K., Richardson, W. D., Bolsover, S. R., and Raff, M. C. (1989) PDGF and intracellular signaling in the timing of oligodendrocyte differentiation. *J. Cell Biol.* **109,** 3411–3417
66. de Laurentiis, A., Donovan, L., and Arcaro, A. (2007) Lipid rafts and caveolae in signaling by growth factor receptors. *Open Biochem. J.* **1,** 12–32
67. Mitsuda, T., Furukawa, K., Fukumoto, S., Miyazaki, H., and Urano, T. (2002) Overexpression of ganglioside GM1 results in the dispersion of platelet-derived growth factor receptor from glycolipid-enriched microdomains and in the suppression of cell growth signals. *J. Biol. Chem.* **277,** 11239–11246
68. Flores, A. I., Mallon, B. S., Matsui, T., Ogawa, W., Rosenzweig, A., Okamoto, T., and Macklin, W. B. (2000) Akt-mediated survival of oligodendrocytes induced by neuregulins. *J. Neurosci.* **20,** 7622–7630
69. Rafalski, V. A., Ho, P. P., Brett, J. O., Ucar, D., Dugas, J. C., Pollina, E. A., Chow, L. M., Ibrahim, A., Baker, S. J., Barres, B. A., Steinman, L., and Brunet, A. (2013) Expansion of oligodendrocyte progenitor cells following SIRT1 inactivation in the adult brain. *Nat. Cell Biol.* **15,** 614–624
70. Hill, M. M., Feng, J., and Hemmings, B. A. (2002) Identification of a plasma membrane Raft-associated PKB Ser473 kinase activity that is distinct from ILK and PDK1. *Curr. Biol.* **12,** 1251–1255
71. Reis-Sobreiro, M., Roué, G., Moros, A., Gajate, C., de la Iglesia-Vicente, J., Colomer, D., and Mollinedo, F. (2013) Lipid raft-mediated Akt signaling as a therapeutic target in mantle cell lymphoma. *Blood Cancer J.* **3,** e118
72. Futter, C. E., Pearse, A., Hewlett, L. J., and Hopkins, C. R. (1996) Multivesicular endosomes containing internalized EGF-EGF receptor complexes mature and then fuse directly with lysosomes. *J. Cell Biol.* **132,** 1011–1023
73. Sandhoff, K., and Klein, A. (1994) Intracellular trafficking of glycosphingolipids: role of sphingolipid activator proteins in the topology of endocytosis and lysosomal digestion. *FEBS Lett.* **346,** 103–107
74. Théry, C., Zitvogel, L., and Amigorena, S. (2002) Exosomes: composition, biogenesis and function. *Nat. Rev. Immunol.* **2,** 569–579
75. Vidal, M., Mangeat, P., and Hoekstra, D. (1997) Aggregation reroutes molecules from a recycling to a vesicle-mediated secretion pathway during reticulocyte maturation. *J. Cell Sci.* **110,** 1867–1877
76. Trajkovic, K., Hsu, C., Chiantia, S., Rajendran, L., Wenzel, D., Wieland, F., Schwille, P., Brügger, B., and Simons, M. (2008) Ceramide triggers budding of exosome vesicles into multivesicular endosomes. *Science* **319,** 1244–1247
77. György, B., Szabó, T. G., Pásztói, M., Pál, Z., Misják, P., Aradi, B., László, V., Pállinger, E., Pap, E., Kittel, A., Nagy, G., Falus, A., and Buzás, E. I. (2011) Membrane vesicles, current state-of-the-art: emerging role of extracellular vesicles. *Cell Mol. Life Sci.* **68,** 2667–2688
78. Marsh, M., and van Meer, G. (2008) Cell biology: no ESCRTs for exosomes. *Science* **319,** 1191–1192
79. Strauss, K., Goebel, C., Runz, H., Möbius, W., Weiss, S., Feussner, I., Simons, M., and Schneider, A. (2010) Exosome secretion ameliorates lysosomal storage of cholesterol in Niemann-Pick type C disease. *J. Biol. Chem.* **285,** 26279–26288
80. Bobrie, A., Colombo, M., Raposo, G., and Théry, C. (2011) Exosome secretion: molecular mechanisms and roles in immune responses. *Traffic* **12,** 1659–1668
81. Verweij, F. J., Middeldorp, J. M., and Pegtel, D. M. (2012) Intracellular signaling controlled by the endosomal-exosomal pathway. *Commun Integr. Biol.* **5,** 88–93
82. Krämer-Albers, E. M., Bretz, N., Tenzer, S., Winterstein, C., Möbius, W., Berger, H., Nave, K. A., Schild, H., and Trotter, J. (2007) Oligodendrocytes secrete exosomes containing major myelin and stress-protective proteins: Trophic support for axons? *Proteomics Clin. Appl.* **1,** 1446–1461
83. Barres, B. A., and Raff, M. C. (1993) Proliferation of oligodendrocyte precursor cells depends on electrical activity in axons. *Nature* **361,** 258–260
84. Demerens, C., Stankoff, B., Logak, M., Anglade, P., Allinquant, B., Couraud, F., Zalc, B., and Lubetzki, C. (1996) Induction of myelination in

the central nervous system by electrical activity. *Proc. Natl. Acad. Sci. U.S.A.* **93,** 9887–9892
85. Fields, R. D. (2006) Nerve impulses regulate myelination through purinergic signalling. *Novartis Found. Symp.* **276,** 148–158; discussion 158–161, 233–147, 275–181
86. Gibson, E. M., Purger, D., Mount, C. W., Goldstein, A. K., Lin, G. L., Wood, L. S., Inema, I., Miller, S. E., Bieri, G., Zuchero, J. B., Barres, B. A., Woo, P. J., Vogel, H., and Monje, M. (2014) Neuronal activity promotes oligodendrogenesis and adaptive myelination in the mammalian brain. *Science* **344,** 1252304
87. Ishibashi, T., Dakin, K. A., Stevens, B., Lee, P. R., Kozlov, S. V., Stewart, C. L., and Fields, R. D. (2006) Astrocytes promote myelination in response to electrical impulses. *Neuron* **49,** 823–832
88. Miron, V. E., Boyd, A., Zhao, J. W., Yuen, T. J., Ruckh, J. M., Shadrach, J. L., van Wijngaarden, P., Wagers, A. J., Williams, A., Franklin, R. J., and ffrench-Constant, C. (2013) M2 microglia and macrophages drive oligodendrocyte differentiation during CNS remyelination. *Nat. Neurosci.* **16,** 1211–1218
89. Kotter, M. R., Setzu, A., Sim, F. J., Van Rooijen, N., and Franklin, R. J. (2001) Macrophage depletion impairs oligodendrocyte remyelination following lysolecithin-induced demyelination. *Glia* **35,** 204–212
90. Baer, A. S., Syed, Y. A., Kang, S. U., Mitteregger, D., Vig, R., Ffrench-Constant, C., Franklin, R. J., Altmann, F., Lubec, G., and Kotter, M. R. (2009) Myelin-mediated inhibition of oligodendrocyte precursor differentiation can be overcome by pharmacological modulation of Fyn-RhoA and protein kinase C signalling. *Brain* **132,** 465–481
91. Haghighi, S., Lekman, A., Nilsson, S., Blomqvist, M., and Andersen, O. (2012) Myelin glycosphingolipid immunoreactivity and CSF levels in multiple sclerosis. *Acta Neurol. Scand.* **125,** 64–70
92. Cafferty, W. B., Duffy, P., Huebner, E., and Strittmatter, S. M. (2010) MAG and OMgp synergize with Nogo-A to restrict axonal growth and neurological recovery after spinal cord trauma. *J. Neurosci.* **30,** 6825–6837
93. Raiker, S. J., Lee, H., Baldwin, K. T., Duan, Y., Shrager, P., and Giger, R. J. (2010) Oligodendrocyte-myelin glycoprotein and Nogo negatively regulate activity-dependent synaptic plasticity. *J. Neurosci.* **30,** 12432–12445
94. Chesley, A., Lundberg, M. S., Asai, T., Xiao, R. P., Ohtani, S., Lakatta, E. G., and Crow, M. T. (2000) The β_2-adrenergic receptor delivers an antiapoptotic signal to cardiac myocytes through G_i-dependent coupling to phosphatidylinositol 3′-kinase. *Circ. Res.* **87,** 1172–1179
95. Marsching, C., Eckhardt, M., Gröne, H. J., Sandhoff, R., and Hopf, C. (2011) Imaging of complex sulfatides SM3 and SB1a in mouse kidney using MALDI-TOF/TOF mass spectrometry. *Anal. Bioanal. Chem.* **401,** 53–64
96. Takahashi, T., Ito, K., Fukushima, K., Takaguchi, M., Hayakawa, T., Suzuki, Y., and Suzuki, T. (2012) Sulfatide negatively regulates the fusion process of human parainfluenza virus type 3. *J. Biochem.* **152,** 373–380
97. Blomqvist, M., Osterbye, T., Månsson, J. E., Horn, T., Buschard, K., and Fredman, P. (2002) Sulfatide is associated with insulin granules and located to microdomains of a cultured β cell line. *Glycoconj. J.* **19,** 403–413
98. Hiraiwa, N., Fukuda, Y., Imura, H., Tadano-Aritomi, K., Nagai, K., Ishizuka, I., and Kannagi, R. (1990) Accumulation of highly acidic sulfated glycosphingolipids in human hepatocellular carcinoma defined by a series of monoclonal antibodies. *Cancer Res.* **50,** 2917–2928
99. Sakakibara, N., Gasa, S., Kamio, K., Makita, A., Nonomura, K., Togashi, M., Koyanagi, T., Hatae, Y., and Takeda, K. (1991) Distinctive glycolipid patterns in Wilms' tumor and renal cell carcinoma. *Cancer Lett.* **57,** 187–192
100. Morichika, H., Hamanaka, Y., Tai, T., and Ishizuka, I. (1996) Sulfatides as a predictive factor of lymph node metastasis in patients with colorectal adenocarcinoma. *Cancer* **78,** 43–47